

RESEARCH

Open Access



Dosimetric comparison of ZAP-X, Gamma Knife, and CyberKnife stereotactic radiosurgery for single brain metastasis

Jinyuan Wang^{1†}, Qingzeng Zheng^{2†}, Yanping Wang^{3†}, Chengcheng Wang¹, Shouping Xu⁴, Zhongjian Ju¹, Longsheng Pan⁵, Jingmin Bai¹, Yunmo Liu⁵, Baolin Qu^{1*} and Xiangkun Dai^{1*}

Abstract

Purpose To evaluate the dosimetric characteristics of ZAP-X stereotactic radiosurgery (SRS) for single brain metastasis by comparing with two mature SRS platforms.

Methods Thirteen patients with single brain metastasis treated with CyberKnife (CK) G4 were selected retrospectively. The prescription dose for the planning target volume (PTV) was 18–24 Gy for 1–3 fractions. The PTV volume ranged from 0.44 to 11.52 cc. Treatment plans of thirteen patients were replanned using the ZAP-X plan system and the Gamma Knife (GK) ICON plan system with the same prescription dose and organs at risk (OARs) constraints. The prescription dose of PTV was normalized to 70% for both ZAP-X and CK, while it was 50% for GK. The dosimetric parameters of three groups included the plan characteristics (CI, GI, GSI, beams, MUs, treatment time), PTV (D_2 , D_{95} , D_{98} , D_{min} , D_{mean} , Coverage), brain tissue (volume of 100%–10% prescription dose irradiation $V_{100\%}$ – $V_{10\%}$, D_{mean}) and other OARs (D_{max} , D_{mean}), all of these were compared and evaluated. All data were read and analyzed with MIM Maestro. One-way ANOVA or a multisample Friedman rank sum test was performed, where $p < 0.05$ indicated significant differences.

Results The CI of GK was significantly lower than that of ZAP-X and CK. Regarding the mean value, ZAP-X had a lower GI and higher GSI, but there was no significant difference among the three groups. The MUs of ZAP-X were significantly lower than those of CK, and the mean value of the treatment time of ZAP-X was significantly shorter than that of CK. For PTV, the D_{95} , D_{98} , and target coverage of CK were higher, while the mean of D_{min} of GK was significantly lower than that of CK and ZAP-X. For brain tissue, ZAP-X showed a smaller volume from $V_{100\%}$ to $V_{20\%}$; the statistical results of $V_{60\%}$ and $V_{50\%}$ showed a difference between ZAP-X and GK, while the $V_{40\%}$ and $V_{30\%}$ showed a significant difference between ZAP-X and the other two groups; $V_{10\%}$ and D_{mean} indicated that GK was better. Excluding the D_{max}

[†]Jinyuan Wang, Qingzeng Zheng and Yanping Wang have contributed equally to this work and share first authorship.

*Correspondence:
Baolin Qu
qubl6212@sina.com
Xiangkun Dai
iabcde@163.com

Full list of author information is available at the end of the article



© The Author(s) 2024. **Open Access** This article is licensed under a Creative Commons Attribution-NonCommercial-NoDerivatives 4.0 International License, which permits any non-commercial use, sharing, distribution and reproduction in any medium or format, as long as you give appropriate credit to the original author(s) and the source, provide a link to the Creative Commons licence, and indicate if you modified the licensed material. You do not have permission under this licence to share adapted material derived from this article or parts of it. The images or other third party material in this article are included in the article's Creative Commons licence, unless indicated otherwise in a credit line to the material. If material is not included in the article's Creative Commons licence and your intended use is not permitted by statutory regulation or exceeds the permitted use, you will need to obtain permission directly from the copyright holder. To view a copy of this licence, visit <http://creativecommons.org/licenses/by-nc-nd/4.0/>.

of the brainstem, right optic nerve and optic chiasm, the mean value of all other OARs was less than 1 Gy. For the brainstem, GK and ZAP-X had better protection, especially at the maximum dose.

Conclusion For the SRS treating single brain metastasis, all three treatment devices, ZAP-X system, CyberKnife G4 system, and GammaKnife system, could meet clinical treatment requirements. The newly platform ZAP-X could provide a high-quality plan equivalent to or even better than CyberKnife and Gamma Knife, with ZAP-X presenting a certain dose advantage, especially with a more conformal dose distribution and better protection for brain tissue. As the ZAP-X systems get continuous improvements and upgrades, they may become a new SRS platform for the treatment of brain metastasis.

Keywords Dosimetric comparison, Stereotactic radiosurgery, ZAP-X, CyberKnife, Gamma Knife, Brain metastasis

Introduction

Stereotactic radiosurgery (SRS) has become an important clinical treatment for intracranial tumors radiotherapy and is used to treat various benign and malignant intracranial tumors and lesions [1, 2]. In the past few decades, various methods have been developed to implement SRS, with the Leksell GammaKnife being one of the earliest stereotactic systems (Elekta Inc., Stockholm, Sweden). It is a specialized intracranial radiosurgery device that uses 192 fixed Cobalt-60 sources to generate isocentric, non-coplanar irradiation [3]. Later, CyberKnife was developed specifically for stereotactic radiation therapy, which achieved nonisocentric and non-coplanar irradiation through robotic arms [4] as well as a treatment platform based on linear accelerators [5]. These devices and methods have their own characteristics and advantages, and there have been many studies related to these devices and methods [6–9].

The ZAP-X stereotactic radiosurgery system (referred to as the ZAP-X system) is new equipment for stereotactic radiosurgery, specifically designed for brain and head and neck tumors. Developed by Stanford University professor John Adler, the inventor of CyberKnife, it is used for the treatment of benign and malignant intracranial lesions. One of the most prominent features of ZAP-X is its fully self-shielding design, which greatly reduces the construction costs of accelerator room [10, 11]. The ZAP-X system uses a 3.0 megavolt (MV) S-band linear accelerator with a dose rate of 1500 MU/min. Compared with CyberKnife and GammaKnife, the ZAP-X system has a medium energy and can meet the requirements of radiotherapy for head and neck tumors. However, the ZAP-X system uses a linear accelerator instead of a radioactive source. The ZAP-X system is similar to a large gyroscope, and its self-shielding design limits its source axis distance to only 45 cm. The shorter source axis distance reduces beam diffusion and helps to reduce radiation outside the field [12], offering dosimetric advantages for intracranial lesions.

To explore the dosimetric characteristics of the ZAP-X system, this study compares SRS treatment plans of ZAP-X, CyberKnife and Elekta ICON Gamma Knife for single

brain metastasis tumors. The comparison focuses on differences in plan quality, efficiency, and dosimetric characteristics of the three devices, providing a reference for the clinical application of the ZAP-X system in the SRS treatment of intracranial tumors.

Materials and methods

Clinical data

Thirteen patients with single brain metastasis treated with CyberKnife in our hospital from December 2018 to January 2020 were selected retrospectively. The prescription dose for the planning target volume (PTV) was 18–24 Gy for 1–3 fractions. The PTV volume ranged from 0.44 to 11.52 cc, with a median volume of 2.57 cc. Patient ages ranged from 32 to 77 years old, with a median age of 56. The gender ratio was 6:7 (Male: Female). Cases included 8 brain metastasis from lung cancer, 1 from liver cancer, 1 from ovarian cancer, 1 from breast cancer, 1 from renal cancer, and 1 from epithelioid angiosarcoma.

Simulation and scanning

All patients were immobilized with a thermoplastic mask of head and neck, positioned in a supine position. Plain and enhanced CT scans were performed using a Siemens CT (SOMATOM Definition AS 64 row), with a slice thickness of 1 mm. The scanning position was head-first supine (HFS), ranging from the top of the skull to the sixth cervical spine. The images were transmitted to the MultiPlan (Ver 4.0.2) planning system (Accuracy, US) via DICOM.

Similarly, patients were maintained in the same position as CT and scanned with a GE 3.0T MRI (GE Discovery MR 750 W, USA) to using enhanced sequences such as BRAVO (brain volume imaging) and CUBE, with a slice thickness of 1 mm. The magnetic resonance images were transmitted to the MultiPlan planning system (Accuracy, US) via DICOM.

Definition of target and organs at risk

The doctor fused the simulated CT images with the BRAVO and CUBE magnetic resonance images. The

Table 1 Patients and basic treatment information

NO.	Gender	Age	Diagnosis	Prescription dose(Gy)	Fractions	Target volume (cc)
1	Female	77	Left posterior temporal lobe brain metastasis of lung cancer	20	2	2.57
2	Female	62	Brain metastasis of adenocarcinoma of the lung	22.5	3	6.2
3	Male	56	Brain metastasis of liver cancer	22	2	2.28
4	Male	65	Left occipital lobe brain metastasis of adenocarcinoma of the lung	24	3	11.52
5	Female	53	Brain metastasis of ovarian cancer	24	3	7.96
6	Male	61	Brain metastasis of adenocarcinoma of the lung	20	1	0.68
7	Male	52	Brain metastasis of adenocarcinoma of the lung	24	3	3.83
8	Female	56	Left frontal lobe brain metastasis of adenocarcinoma of the lung	22	2	0.93
9	Female	56	Left frontal lobe brain metastasis of breast cancer	24	2	0.77
10	Male	48	Left occipital lobe brain metastasis or Renal cancer	21	1	0.44
11	Male	66	Right temporal lobe brain metastasis of lung cancer	22	2	4.54
12	Female	32	Left cerebellar metastasis of epithelioid angiosarcoma	18	1	0.54
13	Female	62	Left frontal lobe brain metastasis of adenocarcinoma of the lung	22.5	3	10.03

Table 2 OAR dose constraints for different treatment fractions

	1 Fraction	2 Fractions	3 Fractions
Brain Stem	$D_{max} < 15$ Gy $V_{10} < 0.5$ cc	$D_{max} < 19.1$ Gy $V_{13} < 0.5$ cc	$D_{max} < 23.1$ Gy $V_{15.9} < 0.5$ cc
Optic Pathway (including optic nerves and optic chiasm)	$D_{max} < 10$ Gy $V_8 < 0.2$ cc	$D_{max} < 13.7$ Gy $V_{11.7} < 0.2$ cc	$D_{max} < 17.4$ Gy $V_{15.3} < 0.2$ cc
Skin	$D_{max} < 27.5$ Gy $V_{25.5} < 10$ cc	$D_{max} < 30.3$ Gy $V_{28.3} < 10$ cc	$D_{max} < 33$ Gy $V_{31} < 10$ cc

tumor target and organs at risk (OARs) were delineated on the fused images. The target included GTV (the area viewed on CT and/or MRI images) and PTV (a three-dimensional extension of GTV by 1.5 mm). The OARs included the brainstem, left/right lens, left/right eye, left/right optic nerve, optic chiasm and brain tissue (delineated according to CT and/or MRI images).

Prescription dose and the dose limits of organs

The prescription dose for the PTV was 18–24 Gy for 1–3 fractions. The detailed information is shown in Table 1.

The OARs involved in the case included brain tissue, brainstem, left/right optic nerve, left/right eye, left/right lens, and optic chiasm. For different treatment fractions, dose constraints for OARs [13] are listed in Table 2.

Treatment plan design and optimization

Using the CyberKnife G4 planning system, the target and OARs of each patient were delineated, and the contours and CT images transferred to the ZAP-X planning system (version 1.8.52) and the ICON planning system Leksell GammaPlan (version 11.1.1). Three medical physicists independently designed the plan according to clinical requirements. The physicist using CyberKnife had over 10 years of experience in plan design, the physicist using ZAP-X had over 3 years of experience, and the physicist using ICON had over 5 years.

For planning design with CyberKnife, fixed collimators were selected for each patient. The number of fields were kept at less than 120, and the prescription dose was normalized to 70%. The Beam Intersection tab was unselected for eyeballs which prevented direct radiation. The number of collimators could be automatically selected as 2 or 3 combinations, and the tracking method used was 6D_Skull tracking, using the inverse planning and ray-tracing calculation algorithm. The optimization parameters of inverse planning for CyberKnife are shown in Fig. 1(a).

For planning design with the ZAP-X system, the principle of selecting collimators (4.0 mm, 5.0 mm, 7.5 mm, 10.0 mm, 12.5 mm, 15.0 mm, 20.0 mm and 25.0 mm) was to prioritize the largest collimator diameter that could cover the tumor, followed by small collimators [14]. ZAP-X TPS could select and create collimators automatically, but manual selection was performed for better distribution. Before collimator selection, a path design was manually done, avoiding potential danger areas and focusing on patient safety, due to the limitations of the shape and space of ZAP-X. Figure 2 shows the path design process and collimator distribution of one ZAP-X plan. The prescription dose was normalized to 70%, and the number of fields was limited to 200, ensuring the treatment time was within a clinically acceptable range. The tracking method was 6D_Skull tracking using the inverse planning and ray-tracing calculation algorithm. The optimization parameters of inverse planning for ZAP-X is shown in Fig. 1(b).

For planning design with the ICON system, the number of shots were manually set based on the size of the target volume and plan complexity. In each shot, appropriate collimators (4 mm, 8 mm, 16 mm, Block) were manually applied to fill 8 sectors, and the dose was normalized to 50%, using the TMR 10 dose calculation method. Each plan aimed to increase target coverage as much as possible while meeting the dose constraints for

VOI Name	Use	Max Dose (cGy)	Boundary Only	Importance Sampling	Voxels per Beam	Skip Factor	# Constraints
PTV	<input checked="" type="checkbox"/>	2857.00	<input type="checkbox"/>	<input type="checkbox"/>	1	1	10506
GTV	<input type="checkbox"/>		<input type="checkbox"/>	<input type="checkbox"/>	1	1	
Right Eye	<input type="checkbox"/>		<input type="checkbox"/>	<input type="checkbox"/>	1	1	
Right Optic Nerve	<input type="checkbox"/>		<input type="checkbox"/>	<input type="checkbox"/>	1	1	
Left Eye	<input type="checkbox"/>		<input type="checkbox"/>	<input type="checkbox"/>	1	1	
Left Optic Nerve	<input type="checkbox"/>		<input type="checkbox"/>	<input type="checkbox"/>	1	1	
Optic Chiasm	<input type="checkbox"/>		<input type="checkbox"/>	<input type="checkbox"/>	1	1	
Brain Stem	<input checked="" type="checkbox"/>	47.00	<input type="checkbox"/>	<input type="checkbox"/>	1	1	51684
[PTV] Shell 1 →Ext. 2mm	<input checked="" type="checkbox"/>	1910.00	<input type="checkbox"/>	<input type="checkbox"/>	1	1	3307
[PTV] Shell 2 →Ext. 5mm	<input checked="" type="checkbox"/>	1240.00	<input type="checkbox"/>	<input type="checkbox"/>	1	1	5186
[PTV] Shell 3 →Ext. 10mm	<input checked="" type="checkbox"/>	760.00	<input type="checkbox"/>	<input type="checkbox"/>	1	1	9282
[PTV] Shell 4 →Ext. 20mm	<input checked="" type="checkbox"/>	390.00	<input type="checkbox"/>	<input type="checkbox"/>	1	1	21791

(a) Optimization parameters of inverse planning for CyberKnife

↑↓	Constraint		≠	Value	Weight
1	PTV	Boundary	≥	2000	10
2	PTV	Interior	≤	2700	70
3	PTV	Ext. (2 mm)	≤	2150	50
4	PTV	Ext. (5 mm)	≤	1200	50
5	PTV	Ext. (10 mm)	≤	800	50
6	Beams		≤	200	

(b) Optimization parameters of inverse planning for ZAP-X

Fig. 1 Optimization parameters of inverse planning for CyberKnife and ZAP-X. (a) CyberKnife optimization parameters. (b) ZAP-X optimization parameters

OARs, ensuring the prescription dose covered over 95% of the PTV.

Dose assessment parameters

To analyze and evaluate the dosimetric characteristics, plan quality, and implementation efficiency of these three pieces of equipment, this study compared and evaluated the plans and the parameters of PTV and the OARs of the three plans based on dose volume histograms (DVH) and dose distribution. The plan parameters included: Paddick conformity index (CI), Paddick gradient index (GI), gradient score index (GSI), beams, total MUs, and treatment time (TT); The PTV parameters included $D_{2\%}$, $D_{95\%}$, $D_{98\%}$, D_{min} , and D_{mean} (normalized to the percentage of prescription dose), Coverage; The OARs parameters included the volume of brain tissue covered by 10 -100%

of prescription dose ($V_{10\%} - V_{100\%}$), D_{mean} of brain tissue, the D_{max} and D_{mean} of the brainstem, bilateral eyes, bilateral lenses, bilateral optic nerves, and optic chiasm.

The paddick conformity index (CI) was defined as $CI = (TVPV \times TVPV)/(TV \times PV)$. TVPV represents the volume of PTV covered by the prescription dose, TV represents the volume of PTV, and PV represents the volume covered by the prescription dose. The maximum value of CI was 1, and the closer it was to 1, the better the conformity of the PTV. If the PTV was covered by the prescription dose line perfectly, the CI was equal to 1, and this plan was an ideal plan [15]. The paddick gradient index (GI) was defined as $GI = PV_{50\%}/PV$. $PV_{50\%}$ represents volume covered by the 50% prescription dose, and PV represents volume covered by the prescription dose. GI was used to reflect the drop in dose outside of PTV in

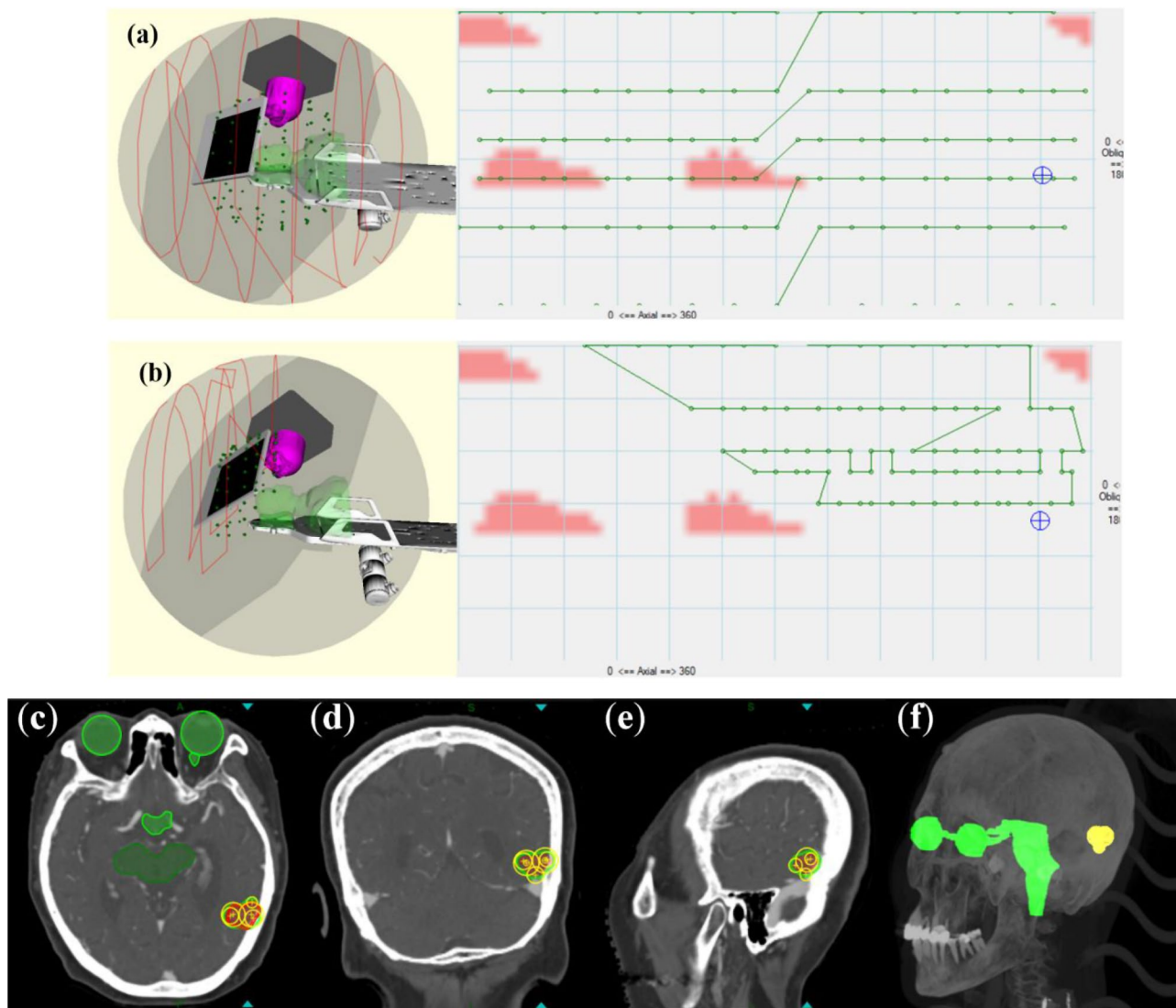


Fig. 2 Path design process and collimator distribution of a Zap-X plan. **(a)** Full gantry delivery positions of the initial path. **(b)** Manually designed gantry delivery positions for each patient avoiding potential danger areas shown in red. **(c)~(e)** Transverse, coronal, and sagittal view of collimator distribution for one ZAP-X plan. Yellow represents the distribution of collimators, red represents the PTV region, and the green thick line around PTV represents the isodose line for prescription dose. **(f)** 3D view of the collimator distribution

terms of volume, and a lower GI indicated a faster drop in dose [15]. The gradient score index (GSI) was defined as $GSI = 100 - 100 \times [(R_{Eff, 50\%Rx} - R_{Eff, Rx}) - 0.3 \text{ cm}]$. $R_{Eff, 50\%Rx}$ and $R_{Eff, Rx}$ represent the equivalent radius when 50% prescription dose volume and prescription dose volume were equivalent to regular spheres. $(R_{Eff, 50\%Rx} - R_{Eff, Rx})$ represents the average distance when the prescription dose dropped to 50%. GSI was used to reflect the drop in dose outside of PTV in terms of distance. When the drop distance was $\leq 3 \text{ mm}$ and the GSI was ≥ 100 , the plan was an ideal plan [16]. The beams refer to the number of radiation fields required in a treatment plan, which could reflect the ability of a planning system to design efficient plans. The total MUs could reflect the workload of the machine. The treatment time (TT) was the beam on time

during a patient's treatment, which could reflect the efficiency of the machine.

Statistical analysis

To avoid statistical errors caused by the differences in software, all data were transmitted to MIM Maestro (version 6.9.5) for processing. Statistical analyses were performed using IBM Statistical Package for Social Sciences (SPSS) software 23.0 (SPSS Inc., Chicago, IL, USA), and the data were expressed as the mean \pm standard deviation. The Shapiro-Wilk normality test was performed for all data, and $p > 0.05$ indicated that it followed a normal distribution. The Levene variance equality test was performed, in which $p > 0.05$ meant that the data had homogeneous variance. If the group of data followed a

Table 3 The planning parameters of ZAP-X, CyberKnife and GammaKnife

	CI	GI	GSI	Beams	Total MUs	TT(min)
ZAP-X	0.81 ± 0.05	2.97 ± 0.23	90.20 ± 12.71	104.85 ± 37.73	11859.73 ± 4897.01	26.00 ± 7.06
CK	0.78 ± 0.07	3.13 ± 0.37	87.58 ± 11.34	108.23 ± 16.58	23089.16 ± 4620.50	38.08 ± 4.54
GK	0.67 ± 0.12	2.97 ± 0.20	87.25 ± 13.58	—*	—*	12.03 ± 5.37
p	<0.001 ^V □○△	0.236 ^V	0.808 ^V	—	—	<0.001 ^V □○△

Notes: □: there was a significant difference between ZAP-X and CK; ○: there was a significant difference between ZAP-X and GK; △: there was a significant difference between CK and GK. *: GK did not have total MUs and beams; V: one-way ANOVA for this group

Table 4 The dosimetric parameters of the PTV in the three groups (%)

	D ₂	D ₉₅	D ₉₈	D _{min}	D _{mean}	Coverage
ZAP-X	136.10 ± 2.27	102.44 ± 1.63	99.41 ± 1.88	88.09 ± 3.79	118.88 ± 1.62	97.43 ± 1.35
CK	140.71 ± 1.72	107.84 ± 1.95	103.89 ± 2.28	90.28 ± 5.25	127.14 ± 6.13	99.19 ± 0.58
GK	188.74 ± 4.66	105.37 ± 4.05	100.37 ± 4.37	81.17 ± 5.60	140.64 ± 4.34	97.80 ± 1.34
p	—	<0.001 ^R □	0.001 ^R □△	<0.001 ^V ○△	—	0.003 ^R □△

Notes: □: there was a significant difference between ZAP-X and CK; ○: there was a significant difference between ZAP-X and GK; △: there was a significant difference between CK and GK. V: one-way ANOVA for this group; R: multiple sample Friedman rank sum tests for this group

Table 5 The dose volume of the brain tissue in the three groups

	ZAP-X	CK	GK	p	ZAP-X	CK	GK	p	
V _{100%} (cc)	4.38 ± 3.97	4.64 ± 4.17	4.93 ± 4.26	0.943 ^V	V _{50%} (cc)	11.80 ± 10.87	12.72 ± 10.90	13.84 ± 12.10	<0.001 ^R ○
V _{90%} (cc)	5.41 ± 4.88	5.65 ± 4.99	6.02 ± 5.17	0.951 ^V	V _{40%} (cc)	15.98 ± 14.95	17.37 ± 14.84	18.62 ± 16.43	0.001 ^R □○
V _{80%} (cc)	6.49 ± 5.83	6.81 ± 5.98	7.29 ± 6.24	0.944 ^V	V _{30%} (cc)	23.89 ± 22.15	26.49 ± 22.32	27.03 ± 23.83	0.003 ^R □○
V _{70%} (cc)	7.74 ± 6.95	8.22 ± 7.15	8.80 ± 7.55	0.932 ^V	V _{20%} (cc)	42.76 ± 37.33	52.92 ± 44.42	45.99 ± 39.96	0.81 ^V
V _{60%} (cc)	9.38 ± 8.50	10.06 ± 8.68	10.85 ± 9.37	0.914 ^V ○	V _{10%} (cc)	131.19 ± 103.68	167.25 ± 122.04	112.01 ± 89.70	0.411 ^V
D _{mean} (Gy)	1.06 ± 0.64	1.12 ± 0.58	0.96 ± 0.64	0.803 ^V					

Notes: □: there was a significant difference between ZAP-X and CK; ○: there was a significant difference between ZAP-X and GK. V: one-way ANOVA for this group; R: multiple sample Friedman rank sum tests for this group

Table 6 Dosimetric parameters of OARs in the three groups (gy)

	ZAP-X	CK	GK	p	ZAP-X	CK	GK	p	
Brain D _{max}	2.33 ± 1.77	3.14 ± 1.77	1.83 ± 1.83	0.074 ^R	Lens-R D _{max}	0.81 ± 1.17	0.19 ± 0.06	0.30 ± 0.26	0.023 ^R □
Stem D _{mean}	0.61 ± 0.49	0.72 ± 0.57	0.53 ± 0.58	0.012 ^R △	Lens-R D _{mean}	0.45 ± 0.52	0.18 ± 0.06	0.20 ± 0.21	0.01 ^R ○
Eye-L D _{max}	0.58 ± 0.43	0.42 ± 0.64	0.46 ± 0.30	0.125 ^R	Optic nerve-L D _{max}	0.92 ± 0.73	0.88 ± 1.18	0.45 ± 0.39	0.009 ^R ○
Eye-L D _{mean}	0.36 ± 0.24	0.20 ± 0.07	0.21 ± 0.18	0.018 ^R ○	Optic nerve-L D _{mean}	0.50 ± 0.37	0.29 ± 0.15	0.27 ± 0.28	0.006 ^R ○
Eye-R D _{max}	0.99 ± 1.34	0.27 ± 0.11	0.51 ± 0.37	0.074 ^R	Optic nerve-R D _{max}	1.20 ± 1.40	0.59 ± 0.74	0.60 ± 0.62	0.056 ^R
Eye-R D _{mean}	0.43 ± 0.41	0.19 ± 0.06	0.23 ± 0.24	0.002 ^R ○	Optic nerve-R D _{mean}	0.55 ± 0.45	0.28 ± 0.16	0.33 ± 0.37	0.037 ^R ○
Lens-L D _{max}	0.45 ± 0.35	0.19 ± 0.06	0.35 ± 0.30	0.092 ^R	Optic chiasma D _{max}	1.71 ± 1.28	1.51 ± 1.57	0.82 ± 0.78	0.146 ^R
Lens-L D _{mean}	0.37 ± 0.29	0.18 ± 0.06	0.20 ± 0.19	0.009 ^R □○	Optic chiasma D _{mean}	0.74 ± 0.58	0.60 ± 0.59	0.47 ± 0.44	0.043 ^R ○

Notes: □: there was a significant difference between ZAP-X and CK; ○: there was a significant difference between ZAP-X and GK; △: there was a significant difference between CK and GK. R: multiple sample Friedman rank sum tests for this group

normal distribution and the variance was homogeneous, one-way ANOVA was used for statistical analysis and LSD was used for posttest in which $p < 0.05$ meant that the data were significantly different; otherwise multiple sample Friedman rank sum tests were applied for statistical analysis; paired multiple comparisons (Bonferroni correction for results) were performed in which $p < 0.05$ meant that the data were significantly different.

Results

According to the analysis, four tables for the ZAP-X, CyberKnife, and GammaKnife are listed: the planning parameters (Table 3), the dosimetric parameters of PTV (Table 4), the dosimetric parameters of the brain tissue

(Table 5) and the dosimetric parameters of other OARs (Table 6).

The planning parameters

The results showed that the CI of GK was significantly lower than that of ZAP-X and CK. For the mean value, ZAP-X and GK had similar GI and were lower than CK, but there was no significant difference among the three groups; meanwhile, ZAP-X had a little higher GSI. The total MUs of ZAP-X were significantly lower than those of CK, and the mean treatment time of ZAP-X was significantly shorter than that of CK; however, there was no significant difference in the beams between the two plans. Due to the use of cobalt-60 sources for GK, the plan and

machine characteristics were different from ZAP-X and CK, and the treatment time was also related to the activity and dose rate of the radiation source; therefore, there were no MUs and beams for GK, and the treatment time of GK only served as a reference.

PTV dosimetry parameters

For PTV, due to the different normalization methods, the D_2 and D_{mean} of GK were higher than those of CK and ZAP-X, as such this group just aimed to show the clinical application characteristics of three devices without statistical comparison. CK had higher D_{95} , D_{98} and coverage (Fig. 3 shows the DVH as an example), indicating that the prescription dose of the CK plan had more sufficient coverage of the PTV. For the minimum dose in PTV, GK was significantly lower than CK and ZAP-X, but their coverage was at a high level, which could meet the quality requirement of clinical treatment plans.

The dose volume of the brain tissue

In the study of the volume corresponding to different doses of brain tissue, it was found that in the volume irradiated at 100% -30% of prescription dose, the mean irradiated volume of ZAP-X < CK < GK. There was no significant difference among the three groups of $V_{100\%}$ - $V_{70\%}$; the statistical results of $V_{60\%}$ and $V_{50\%}$ showed

that there was a significant difference between ZAP-X and GK; the statistical results of $V_{40\%}$ and $V_{30\%}$ showed a significant difference between ZAP-X and the other two groups. For the results of $V_{20\%}$ and $V_{10\%}$, the average irradiation volume of CK was larger than that of the other two groups. ZAP-X showed the smallest irradiation volume in $V_{20\%}$, while GK showed the smallest irradiation volume in $V_{10\%}$, but there was no significant difference among the three groups. For D_{mean} , the average value of GK was smaller, but the three groups were at lower levels with no significant difference. Figure 4 shows the dose distribution of ZAP-X, CK, and GK for a same plan, which could display the difference intuitively in the dose distribution of the three groups.

Dosimetric parameters of other OARs

The average values of the evaluation results were less than 1 Gy, except for the D_{max} of the brainstem, right optic nerve and optic chiasm. For the brainstem, the average values of D_{max} and D_{mean} showed GK < ZAP-X < CK; for the bilateral eyes, bilateral lenses, and right optic nerve, the average values of D_{max} and D_{mean} showed CK < GK < ZAP-X; for the left optic nerve and optic chiasm, the average values of D_{max} and D_{mean} showed GK < CK < ZAP-X. Statistical analysis showed that there was a significant difference

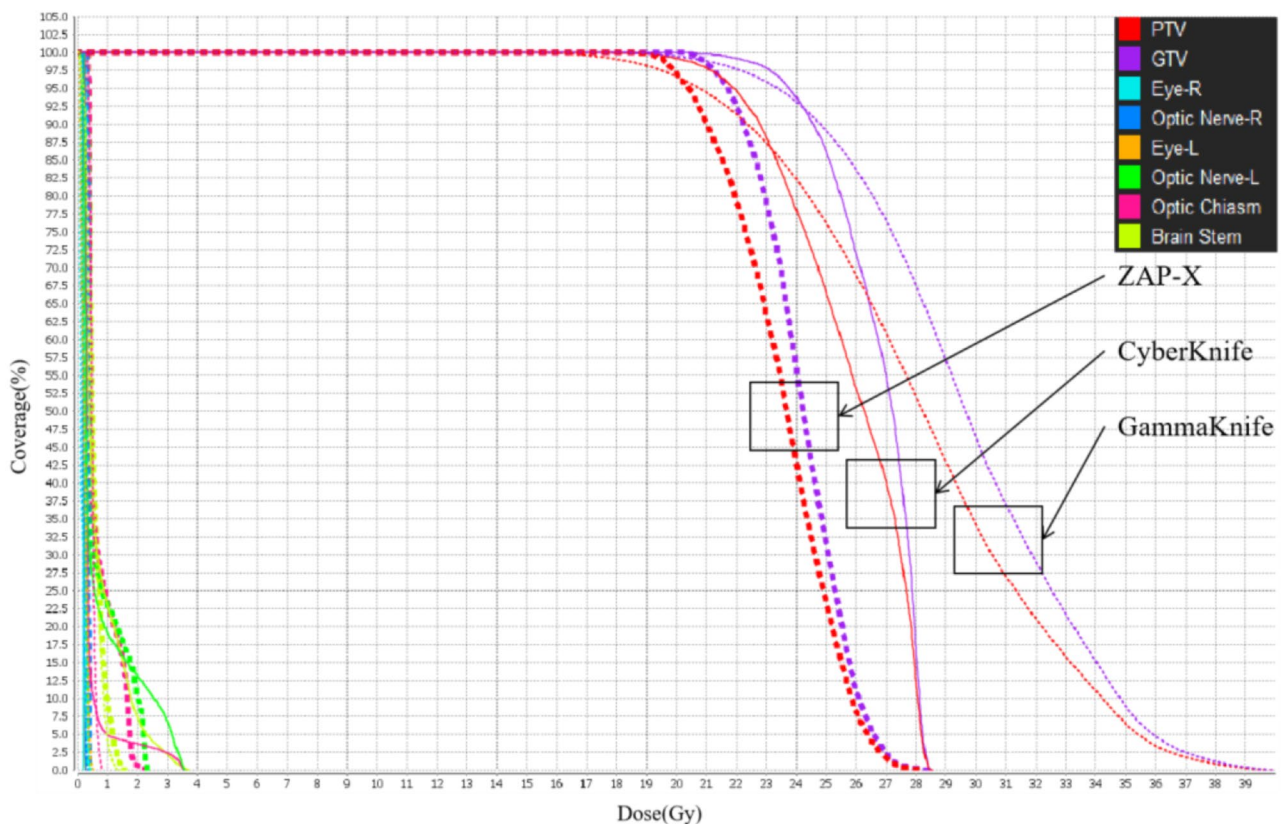


Fig. 3 Comparison between ZAP-X, CyberKnife and GammaKnife of DVH

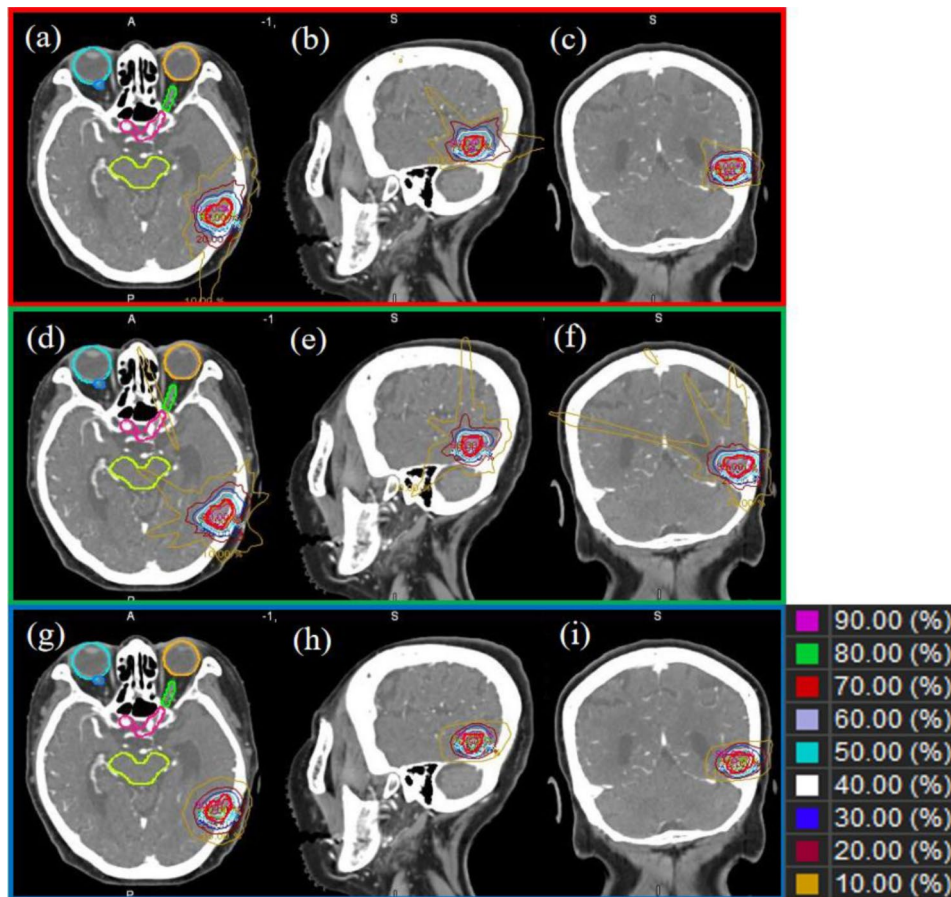


Fig. 4 The isodose distribution of ZAP-X, CyberKnife and GammaKnife. Figures in the red box (a~c) show the dose distribution of ZAP-X, those in the green box (d~f) show the dose distribution of CyberKnife, and those in the blue box (g~i) show the dose distribution of GammaKnife.

between GK and CK in the D_{mean} of the brainstem; the D_{mean} of the bilateral eyes, bilateral lenses, bilateral optic nerves, optic chiasm and the D_{max} of the left optic nerve showed that GK and ZAP-X were significantly different; and the D_{mean} of the left lens and the D_{max} of the right lens showed a significant difference between CK and ZAP-X.

Discussion

With the continuous development of early screening, imaging technology, and treatment technology, the survival rate and quality of life of cancer patients has improved significantly. However, approximately 20-40% of cancer patients still experience brain metastasis [17]. Brain metastasis may occur in the brain parenchyma, pia mater, dura mater and skull. The poor prognosis of patients with brain metastasis may lead to neurological defects, such as seizure, paralysis and cognitive decline, which will greatly reduce the patient life quality [18]. The SRS concept was introduced by Leksell in the 1950s [19], and so far, SRS has been proven to be a safe and effective primary treatment for intracranial metastasis [20, 21]. The SRS treatment

has some characteristics: highly conformal dose distribution, steep dose drop-off gradient, accurate patient positioning, high dose-per-fraction and low fractionation. While ensuring the dose distribution, conformability, and coverage, it provides maximum protection to surrounding normal organs. Therefore, SRS can potentially reduce the intracranial toxicity associated with radiation therapy and improve the tumor local control rate [22, 23].

This study designed and analyzed treatment plans using the ZAP-X system, CyberKnife G4 system, and GammaKnife system for 13 patients with single brain metastasis who had already received CyberKnife treatment. The results indicated that the plan of the three treatment platforms could meet clinical treatment requirements, with sufficient target coverage, steep dose drop-off, and safe OAR doses, but there were some differences among the three groups. Among all plans, ZAP-X and CK got a higher CI than GK, while ZAP-X and GK achieved a lower GI than CK. ZAP-X had a higher CI, higher GSI and a GI comparable to that of Gamma Knife, which is often seen as the “gold standard” in SRS. For PTV, the coverage, D_{95} , D_{98} of CK

were higher than that of ZAP-X and GK, and ZAP-X and GK were about the same except for the D_{\min} of PTV. For ZAP-X, the average D_{\min} of PTV reached 88.09% of the prescription dose, much higher than 81.17% for GK, which indicated that ZAP-X had a more comprehensive irradiation to the PTV compared to GK. In terms of treatment efficiency, the total MUs of ZAP-X were significantly lower than those of CyberKnife, and the treatment time of ZAP-X was shorter. For institutions with heavy treatment load, the high efficiency of ZAP-X could treat more patients. For the average volume of brain tissue covered by 20–100% prescription dose, ZAP-X was surprisingly smaller than CK and GK. This indicated that ZAP-X had a faster dose drop-off, while the volume covered by the 10% prescription dose was higher than that of GK, which should be due to more isocenters and beams of ZAP-X. GK might be more advantageous for $D_{\text{mean}}, V_{10\%}$ (approximately 200 cGy) or lower dose volumes. For the protection of OARs, GK and ZAP-X had better protection for the brainstem than CK, especially the maximum dose, which was consistent with the better GI of GK and ZAP-X. In terms of other OARs, GK and CK were better than ZAP-X due to ZAP-X system did not have the function of allowing radiation to avoid organs, and the GK and CK planning systems both had a blocking function that prevented beams from passing through organs directly. The D_{\max} and D_{mean} for OARs in the three groups were at very low levels because the PTV of the single brain metastasis selected in this study was far from the OARs; for example, the centroid deviation was 4.26–9.16 cm between the brainstem and the PTV.

ZAP-X showed good planning results, with a fast dose drop-off, good conformability, and high treatment efficiency. Studies by Weidlich et al. [24]. and Pinnaduwege et al. [25]. showed that ZAP-X had a smaller penumbra. According to the measurement of the author's previous research, the maximum penumbra of the 25 mm collimator was only 2.42 mm and 2.83 mm at depths of 5 cm and 10 cm, respectively [12]. The radiation leakage of ZAP-X was approximately 0.001%, which meant that the ZAP-X system could provide more radiation to the target and reduce the radiation reaching outside the target. At the same time, due to the low energy and small source axis distance of the ZAP-X system, the beam penumbra was small, the dose drop-off was fast, and it could protect the surrounding organs better. In addition, during the ZAP-X system treatment, the patient was directly fixed on the couch, reducing the error caused by the application of the positioning frame used in other machines, which was beneficial for improving the accuracy.

Benjamin K et al. [26]. and Pan et al. [27]. analyzed the data of patients who received the treatment of the first and second ZAP-X systems. The results showed that SRS treatment with ZAP-X appeared to be safe and effective. These initial clinical reports proved the efficacy and clinical feasibility of ZAP-X in treating intracranial and head and neck tumors. Dosimetric comparison between ZAP-X and CyberKnife for trigeminal neuralgia treatment would determine whether ZAP-X was suitable for high-dose therapy. Pantaleo Romanelli et al [28] made a preliminary dosimetric comparison between ZAP-X and CyberKnife for a patient with trigeminal neuralgia, and the study found that the two plans had the same quality. The reduction in the low dose volume of ZAP-X in this study was consistent with our research results. These preliminary results might prove that ZAP-X has potential clinical value in SRS treatment, but more cases are still needed to prove its long-term efficacy.

There were also limitations in our study. We only conducted preliminary dosimetry studies on single brain metastases, with a single disease and low planning complexity, and there was a considerable distance between the OARs and target. Another limitation was the experience and planning priorities of physicists. All the plans in our study were not designed automatically by TPS but by physicists, while each physicist was dedicated to use different TPS systems, and designed plan with certain priorities based on clinical requirements and their experiences. The general planning goals usually were to ensure target coverage and minimize OAR dose volumes and GI values. However, the plan designing was mostly based on the physicists' years of clinical experience, and the strategies used in the planning, which are inevitably different. All of the three SRS platforms provided satisfactory treatment plans, but we noted that ZAP-X had excellent dose drop-off and better protection of the brain tissue through comprehensive comparison. The ZAP-X used in this study was a first-generation model, and there were limitations in its TPS software. We believe that with the update of TPS, the user experience and plan designing efficiency of ZAP-X would be improved significantly. In addition, as specialized equipment for head and neck radiation surgery, ZAP-X's clinical application may be limited in certain treatment areas.

Conclusions

For the SRS treatment of single brain metastasis, all three treatment platforms, ZAP-X system, CyberKnife G4 system, and GammaKnife system, could meet clinical treatment requirements. ZAP-X could provide high-quality plans that were comparable or even superior to CyberKnife, especially in reducing treatment

time. Compared to Gamma Knife, the more conformal dose distribution and better brain tissue protection in ZAP-X provide a certain dose advantage. Additionally, ZAP-X's savings in the replacement and protection of radiation sources make it safer and more convenient for practical clinical applications. With the continuous improvement and upgrading of the ZAP-X system, it may become a new SRS platform for treating brain metastasis. However, as a new type of stereotactic radiosurgery equipment, the deeper dosimetric characteristics and broader clinical applications of ZAP-X still require further exploration with a larger number of patient cases and disease types to establish more reliable data as a reference for clinical applications.

Author contributions

JW, QZ and YW designed the work and wrote the manuscript. CW, JB and YL collected the data and performed the data analyses. SX, ZJ and LP interpreted the results of the data analyses. BQ and XD provided suggestion for the study, reviewed and revised the article. All authors contributed to the manuscript and approved the final submitted version.

Funding

This work was supported by the National Key Research and Development Program of China (2022YFC2409501).

Data availability

The datasets used and/or analyzed for the current study available from the corresponding author upon reasonable request.

Declarations

Ethical approval and consent to participate

This study was approved by the Medical Ethics Committee of PLA General Hospital (EC Approval #2019022), and informed consents were obtained from all subjects.

Consent to publish

Not applicable.

Competing interests

The authors declare no competing interests.

Author details

¹Department of Radiation Oncology, The First Medical Center of PLA General Hospital, Beijing 100853, China

²Department of Radiotherapy, Beijing Geriatric Hospital, Beijing 100095, China

³Department of Radiation Oncology, Hebei Yizhou Cancer Hospital, Zhuozhou 072750, China

⁴National Cancer Center, National Clinical Research Center for Cancer/Cancer Hospital, Chinese Academy of Medical Sciences and Peking Union Medical College, Beijing 100021, China

⁵Department of Neurosurgery, the First Medical Center of PLA General Hospital, Beijing 100853, China

Received: 15 September 2023 / Accepted: 26 July 2024

Published online: 01 August 2024

References

- Fatima N, Meola A, Ding VY, et al. The Stanford stereotactic radiosurgery experience on 7000 patients over 2 decades (1999–2018): looking far beyond the scalpel[J]. *J Neurosurg*. 2021;135:1721–45. <https://doi.org/10.3171/2020.9.JNS201484>.
- Yang I, Udawatta M, Prashant GN, et al. Stereotactic radiosurgery for neurosurgical patients: a historical review and current perspectives[J]. *World Neurosurg*. 2019;122:522–31. <https://doi.org/10.1016/j.wneu.2018.10.193>.
- Lindquist C, Paddick I. The Leksell Gamma Knife Perfexion and comparisons with its predecessors[J]. *J Neurosurg*. 2008;62:721–31. <https://doi.org/10.1227/01.neu.0000289726.35330.8a>.
- Gong HS, Ju ZJ, Xu SP, et al. G4 CyberKnife: New Instrument for Stereotactic Radiosurgery and its clinical Application[J]. *Chin Med Equip J*. 2013;34(4):127–9. <https://doi.org/10.7687/J.ISSN1003-8868.2013.04.127>.
- Mitsumori M, Shrieve DC, Alexander E 3rd et al. Initial clinical results of LINAC-based stereotactic radiosurgery and stereotactic radiotherapy for pituitary adenomas[J]. *Int J Radiat Oncol Biol Phys* 1998;42:573–80. [https://doi.org/10.1016/s0360-3016\(98\)00256-9](https://doi.org/10.1016/s0360-3016(98)00256-9).
- Mindermann T, Gamma, Knife. CyberKnife or micromultileaf collimator LINAC for intracranial radiosurgery[J]. *Acta Neurochir*. 2014;157(4):557–8. <https://doi.org/10.1007/s00701-014-2275-6>.
- Blamek S, Grzadziel A, Miszczyk L. Robotic radiosurgery versus micromultileaf collimator: a dosimetric comparison for large or critically located arteriovenous malformations[J]. *Radiat Oncol*. 2013;8:205–13. <https://doi.org/10.1186/1748-717X-8-205>.
- Gevaert T, Levivier M, Lacomberie T, et al. Dosimetric comparison of different treatment modalities for stereotactic radiosurgery of arteriovenous malformations and acoustic neuromas[J]. *Radiother Oncol*. 2013;106:192–7. <https://doi.org/10.1016/j.radonc.2012.07.002>.
- Dutta D, Subramanian SB, Murli V, et al. Dosimetric comparison of Linac-based (BrainLAB) and robotic radiosurgery (CyberKnife) stereotactic system plans for acoustic schwannoma[J]. *J Neurooncol*. 2012;106(3):637–42. <https://doi.org/10.1007/s11060-011-0703-5>.
- Weidlich GA, Schneider M, Adler JR. Self-shielding analysis of the Zap-X system[J]. *Cureus*. 2017, 9(12): e1917. <https://doi.org/10.7759/cureus.1917>
- Cao Q, Tan J, Ren Y et al. Evaluation of Radiation shielding requirements and self-shielding characteristics for a Novel Radiosurgery. *System[J] Health Phys* 2021, 121(5):506–12. <https://doi.org/10.1097/HP.0000000000001465>
- Wang JY, Dai XK, Zheng QZ, et al. A novel stereotactic radiosurgery system Zap-X[J]. *Chin J Med Phys*. 2022;39(1):76–80. <https://doi.org/10.3969/j.issn.1005-202X.2022.01.013>.
- Timmerman R. A story of Hypofractionation and the table on the Wall[J]. *Int J Radiat Oncol Biol Phys*. 2022;112(1):4–21. <https://doi.org/10.1016/j.ijrobp.2021.09.027>.
- Adler JR, Schweikard A, Achkire Y, et al. Treatment planning for self-shielded radiosurgery[J]. *Cureus*. 2017;9(9):e1663. <https://doi.org/10.7759/cureus.1663>.
- Paddick I, Lippitz B. A simple dose gradient measurement tool to complement the conformity index[J]. *J Neurosurg*. 2006;105:194–201. <https://doi.org/10.3171/sup.2006.105.7.194>.
- Wagner TH, Bova FJ, Friedman WA, et al. A simple and reliable index for scoring rival stereotactic radiosurgery plans[J]. *Int J Radiat Oncol Biol Phys*. 2003;57(4):1141–9. [https://doi.org/10.1016/s0360-3016\(03\)01563-3](https://doi.org/10.1016/s0360-3016(03)01563-3).
- Mehta MP, Tsao MN, Whelan TJ et al. The American society for therapeutic radiology and oncology (ASTRO) evidence-based review of the role of radiosurgery for brain metastasis[J]. *Int J Radiat Oncol Biol Phys* 2005;63:37–46. <https://doi.org/10.1016/j.ijrobp.2005.05.023>
- Sacks P, Rahman M. Epidemiology of Brain Metastases[J]. *Neurosurg Clin N Am*. 2020;31(4):481–8. <https://doi.org/10.1016/j.nec.2020.06.001>.
- Leksell L. The stereotactic method and radiosurgery of the brain[J]. *Acta Chir Scand*. 1951;102:316–9.
- Traylor JJ, Habib A, Patel R, et al. Fractionated stereotactic radiotherapy for local control of resected brain metastases[J]. *J Neurooncol*. 2019;144:343–50. <https://doi.org/10.1007/s11060-019-03233-9>.
- Mazzola R, Corradini S, Gregucci F et al. Role of radiosurgery/stereotactic radiotherapy in oligometastatic disease: brain oligometastases[J]. *Front Oncol*, 2019;9:206. <https://doi.org/10.3389/fonc.2019.00206>
- Alongi F, Fiorentino A, Gregucci F et al. First experience and clinical results using a new noncoplanar monoisocenter technique (HyperArc™) for Linac-based VMAT radiosurgery in brain metastases[J]. *J Cancer Res Clin Oncol* 2019, 145:193–200. <https://doi.org/10.1007/s00432-018-2781-7>
- Ruggieri R, Naccarato S, Mazzola R et al. Linac-based VMAT radiosurgery for multiple brain lesions: comparison between a conventional multi-isocenter approach and a new dedicated mono-isocenter technique[J]. *Radiat Oncol*, 2018, 13:38. <https://doi.org/10.1186/s13014-018-0985-2>
- Weidlich GA, Chung W, Kolli S et al. Characterization of the ZAP-X® peripheral dose fall-off[J]. *Cureus*, 2021, 13(3): e13972. <https://doi.org/10.7759/cureus.13972>

25. Pinnaduwaage DS, Srivastava SP, Yan XS et al. Small- field beam data acquisition, detector dependency, and film-based validation for a novel self- shielded stereotactic radiosurgery system[J]. *Med Phys* 2021,48: 6121–36<https://doi.org/10.1002/mp.15091>
26. Hendricks BK, DiDomenico JD, Barani IJ et al. ZAP-X gyroscopic radiosurgery system: a preliminary analysis of clinical applications within a Retrospective Case Series[J]. *Stereotact Funct Neurosurg* 2022,100(2):99–107<https://doi.org/10.1159/000519862>
27. Pan L, Qu B, Bai J, et al. The Zap-X radiosurgical system in the treatment of intracranial tumors: a technical case report[J]. *J Neurosurg.* 2021;88(4):E351–E. <https://doi.org/10.1093/neuros/nyaa550>. 355.
28. Romanelli P, Chuang C, Meola A et al. ZAP-X: a Novel Radiosurgical device for the treatment of trigeminal Neuralgia[J]. *Cureus*,2020,12(5):e8324. <https://doi.org/10.7759/cureus.8324>

Publisher's Note

Springer Nature remains neutral with regard to jurisdictional claims in published maps and institutional affiliations.